THE JOURNAL OF PHYSICAL CHEMISTRY B

Article

pubs.acs.org/JPCB

Monitoring the Electrophoretic Migration and Adsorption of Single Insulating Nanoparticles at Ultramicroelectrodes

Aliaksei Boika,[†] Scott N. Thorgaard,[†] and Allen J. Bard*

Center for Electrochemistry, Department of Chemistry and Biochemistry, University of Texas at Austin, Welch Hall 2.204, 105 East 24th Street Stop A5300, Austin, Texas 78712-1224, United States

Supporting Information

ABSTRACT: The individual adsorption events of sub-μm silica and polystyrene spheres (310−530 nm in diam.) were detected by monitoring the blocking of redox mediator diffusion to Pt ultramicroelectrode (UME) substrates by the adsorbing spheres. Under the diffusion limited oxidation of FcMeOH and at low supporting electrolyte concentrations, the negatively charged spheres arrive at the electrode by electrophoretic migration. Sphere adsorption monitoring experiments consisted of long-time (1000−5000 s) chronoamperograms recorded in solutions with fM concentrations of spheres and different concentrations of supporting electrolyte. Trends in the heights of the step features with time reflect changing surface coverage of spheres, and coupled step features in the chronoamperograms suggest dynamic rearrangement of spheres on the surface. Numerical simulations of diffusion blocking at electrodes by adsorbing particles as well as mass transport of particles under migration were also performed, and show good agreement with the experimental data collected.

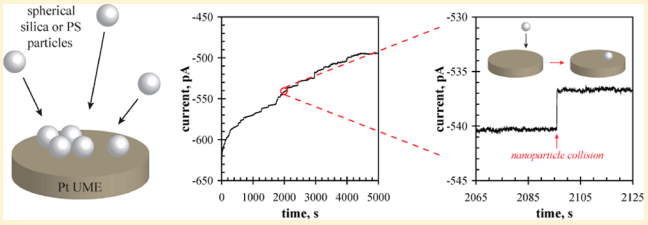

INTRODUCTION

Quinn, van't Hof, and Lemay (QHL) found that the adsorption events of single insulating particles could be observed by their blocking of the electron transfer of a diffusing redox species to an ultramicroelectrode (UME).[1] Their work fits into a larger subfield of single nanoparticle (NP)/electrode collision studies, in which individual particle impact events on surfaces have been detected electrochemically under potentiostatic conditions. While earlier, "ensemble level" works in NP electrochemistry by Heyrovsky et al.[2−5] investigated the effect of NPs on cyclic voltammetry (CV), follow up efforts by Scholz[6−8] and Compton[9,10] detected collisions of single μm-scale or nm-scale particles either by their individual charging current flows during impacts or by their perturbation of the substrate electrode double layer capacitance. Our group's approach has been based on electrocatalysis where NPs being detected catalyze an electron transfer reaction of a diffusing species which does not occur on the underlying substrate electrode.[11−15] In this way, the conductive NP in contact with the surface functions as a tiny working electrode for the electron transfer reaction, while the inert substrate serves as a bridge to allow the flow of electrons to the external circuit. Although this approach allows for a great improvement in measurement sensitivity due to the amplification offered by the electrocatalytic effect, it requires conductive NPs. Compton's group has also recorded individual particle/electrode interactions by electron transfer reactions directly involving the particle material or particle surface, such as for the total oxidation of single Ag particles.[16]

On the other hand, QHL observed the adsorption events of single carboxlyated latex beads as well as CdSe NPs by their blocking the electrode reaction of ferrocenemethanol (FcMeOH) to Au UMEs.[1] The particles arrived at the electrode by electrophoretic migration, and the authors investigated the dependence of the arrival rate on the electrode current and the supporting electrolyte concentration.

As the blocking of redox mediator electrochemistry occurs without any electrochemistry of the particles, this technique enables the use of electrochemical methods to monitor collisions of insulating NPs. In the present work, we have extended this approach to observe the adsorption events of single silica and polystyrene nanospheres at Pt UMEs. These results extend the techniques of QHL to these new materials, and further illustrate the utility of simultaneously monitoring NP adsorption by diffusion blocking and directing the arrival of NPs at an UME substrate using electrophoretic migration. Moreover, we have performed numerical simulations of both blocking by individual spheres and the flux of spheres to the working electrode under migration. QHL also used finite element calculations to model the expected blocking of FcMeOH diffusion by one adsorbed sphere for set sphere and electrode dimensions. However, in our approach, we carry out simulations for an insulating ring on the surface of an

Special Issue: Paul F. Barbara Memorial Issue

Received: July 13, 2012
Revised: October 16, 2012
Published: October 23, 2012

ACS Publications © 2012 American Chemical Society

Table 1. Comparison of Experimental and Simulated Values of Collision Frequency for Different Systems

system	ζ-potential (particle) (mV)	electric field (edge) (V/m)	f (simulated) (Hz)	f (experimental) (Hz)
PS 520 nm (unmodif.), 1 mM KCl, 0.45 V	−66.7 ± 10.5	9.56×10^4	0.28 ± 0.03	0.24 ± 0.06
PS 520 nm (unmodif.), 1 mM KCl, 0.28 V		3.37×10^4	0.16 ± 0.02	0.11 ± 0.02
PS 520 nm (unmodif.), 5 mM KCl, 0.45 V	−52.8 ± 11.3	3.16×10^4	0.052 ± 0.010	0.073 ± 0.025
PS 520 nm (unmodif.), 5 mM KCl, 0.28 V		0.89×10^4	0.026 ± 0.005	0.031 ± 0.002
PS 530 nm (−COOH), 1 mM KCl, 0.45 V	−66.9 ± 6.5	9.56×10^4	0.28 ± 0.02	0.30 ± 0.06
silica, 310 nm, 1 mM KCl, 0.5 V	−58.9 ± 8.4	1.70×10^5	0.11 ± 0.02	0.078 ± 0.006
silica, 310 nm, 5 mM KCl, 0.5 V	−50.8 ± 8.1	0.61×10^5	0.024 ± 0.004	0.017 ± 0.004

electrode and then do a recalculation of the results for a single particle.

In this publication, we also present a theoretical model that simulates the mass transfer of insulating spheres to an electrode. This model is unique in a sense that it allows simulation of the electric field responsible for sphere migration. Therefore, the theoretical description of the migration phenomena that we developed in the course of this work extends substantially the early report by QHL.

■ EXPERIMENTAL SECTION

Materials and Instrumentation. The spherical particles used in adsorption experiments shown were commercially available, unmodified silica spheres (310 nm diam.), unfunctionalized polystyrene (520 nm diam.), and carboxylated polystyrene (530 nm diam.), all purchased as monodisperse aqueous suspensions from Bangs Laboratories, Inc. (Fishers, IN; catalog numbers SS02N, PS03N, and PC03N, respectively). The polystyrene spheres were supplied in solutions containing sodium dodecyl sulfate and sodium azide. To remove these compounds, the polystyrene spheres were washed with pure water and centrifuged twice before experiments. All solutions were prepared with deionized water and charcoal treated using a Millipore purification system (Millipore, Bedford, MA). Commercially available FcMeOH, purchased from Alfa Aesar (Ward Hill, MA), as well as KCl and H_2SO_4 from Fisher Scientific (Hampton, NH) were each used as received. ζ-Potential measurements of the spheres were carried out using a Malvern Zetasizer dynamic light scattering instrument (Malvern Instruments, Ltd., Malvern, Worcestershire, U.K.). All ζ-potentials were measured for dilute (pM concentration) aqueous suspensions of the spheres with supporting electrolyte concentrations, as listed in Table 1.

Electrochemical data shown for silica sphere adsorption were recorded using a CH920c scanning electrochemical microscope (CH Instruments, Austin, TX) in a three-electrode configuration. Experiments involving polystyrene spheres were performed using a two-electrode configuration, which consisted of a Chem − Clamp instrument (Dagan Corporation), Model 175 Universal Programmer (Princeton Applied Research), and a DAQ card (National Instruments NI PCI-6251) for data acquisition with LabView software. The data acquisition rate for the chronoamperometric measurements was 10 Hz (Chem − Clamp instrument). For both instrumental setups, the noise was estimated to be roughly ≤0.2 pA peak-to-peak; a sample chronoamperogram is shown in Figure S1 in the Supporting Information. Thus, sudden changes recorded in the steady state current ("step" features occurring over 1−3 data points) with magnitudes of at least 1.5−2 times the noise amplitude (0.3−0.4 pA) were counted as particle collisions. For sphere adsorption data, reported frequency values in Hz for step events were calculated by dividing the total number of steps by the observation time in s. As described below, slightly different, but complementary, procedures were used for the silica and polystyrene sphere adsorption experiments. In both cases, no deaeration of the experimental cells was required because the oxidation of FcMeOH is insensitive to oxygen.

Silica Sphere Adsorption Experimental Procedure. The working electrode for silica sphere experiments was a 2 μm diameter Pt disk fabricated by sealing a Pt microwire, which was sharpened by anodization in aqueous 60% (by volume) saturated $CaCl_2$ with 4% concentrated HCl, and sealed in a glass capillary and then exposing a Pt disk by grinding.[17] Because of nonuniformity in the cross-sectional area of the etched microwire along its apex, the active surface area of the working electrode varied slightly between experiments because of its repolishing. Bright Pt wires served as both quasi-reference and auxiliary electrodes for sphere adsorption experiments; however, the potential of the Pt quasi-reference electrode was verified by CV using a Ag/AgCl reference electrode (3 M KCl, AgCl saturated inner filling solution; glass frit separation from sample), and all potentials in this work are quoted with respect to the Ag/AgCl reference electrode. All chronoamperometry was performed with the working electrode potential set to +0.5 V, roughly 0.2 V positive of the half wave potential for FcMeOH oxidation as measured by CV. This value was chosen deliberately to minimize the effect of any drift in the quasi-reference electrode and to ensure that sphere adsorption occurred under diffusion limited oxidation of FcMeOH.

Before each experiment, the working electrode was gently polished on fine sandpaper (1200 Grit (P2500) MicroCut Discs, Buehler, Lake Bluff, IL) and then sonicated in pure water for 3 min. The electrode was then subjected to electrochemical cleaning by potential cycling in 0.34 M H_2SO_4 for 1 h, rinsed in pure water, and immediately introduced into the experimental cell. Care was taken to avoid contamination of the cell with stray particles, e.g., from polishing, dust, or silica spheres from earlier experiments. Each experiment was performed in a closed glass cell consisting of a disposable glass vial with a PTFE cover. Glass vials were initially cleaned by rinsing with copious amounts of pure water followed by drying in an oven, and were not reused between experiments. Before filling the cell, FcMeOH/KCl solutions were filtered through an additional 0.2 μm PTFE filter (Autovial, Whatman, Florham Park, NJ) to remove particles that may have been introduced during solution preparation. In experiments carried out under conditions where dust/particle contamination was suspected (e.g., with an open-topped cell, unfiltered solutions, or when extensive polishing of the electrode with alumina powders had been attempted), small numbers (<5 per 1000 s) of irregular step features in the chronoamperometry data were occasionally observed. We have interpreted these steps as blocking of the electrode by irreversibly adhering contaminating particles. Therefore, as a check of solution cleanliness, 1000 s of chronoamperometry

data was always recorded before addition of the spheres. For all experiments described, no steps were observed before the introduction of silica spheres.

A stock suspension of the spheres (5 pM) was prepared in pure water and then added to the experimental cell by autopipette to produce the concentrations listed. In order to reduce the likelihood of sphere aggregation in the experimental cell, the stock sphere suspension was sonicated for 15 min prior to addition to the cell. Injection of the spheres was performed at open circuit (no applied potential), after which the cell was gently stirred for 30 s followed by a 10 min wait to establish a uniform concentration of spheres in the cell before the chronoamperometry data were collected. No gravitational settling of the spheres was observed in the stock over several hours.

Polystyrene Sphere Adsorption Experimental Procedure. For polystyrene sphere adsorption experiments, a 5 μm diameter Pt disk UME was used as the working electrode, and a conventional Ag|AgCl||KCl(sat.) electrode served both as the reference and counter electrodes (two-electrode cell). Before each experiment a steady-state CV corresponding to the diffusion limited oxidation of FcMeOH was recorded to confirm the stability and quality of the setup. Polystyrene spheres were diluted to a concentration of 21.2 pM to achieve the desired final concentration in the electrochemical cell once injected. The collision curve was recorded as follows: first, a chronoamperogram was recorded at +0.45 V (diffusion limited oxidation of FcMeOH) for 5 min in the absence of polystyrene particles. Then, the potential of the working electrode was stepped to 0 V where no oxidation of FcMeOH took place. Immediately after that, an aliquot of the diluted aqueous suspension of polystyrene particles was injected and the solution agitated with an argon flow for at least 10 s to disperse the particles uniformly throughout the whole volume of the cell. The potential of the working electrode was then stepped back to its initial value (+0.45 V), and the collision events were recorded for at least 1000 s. Obtained data were further analyzed in terms of the magnitude of the current steps and their frequency. While the injection of particles at 0 V here for polystyrene spheres differs from the injection at an open circuit as used for silica spheres, these procedures should be equivalent because both were performed under zero-current conditions. As explained further below, negligible sphere adsorption occurs in the absence of current due to the very slow diffusion of the spheres.

■ RESULTS AND DISCUSSION

Adsorption Experiments with Insulating Spheres. Shown in Figure 1 are chronoamperograms recorded for a Pt UME (diameter = 2 μm) immersed in a solution containing 2.5 mM FcMeOH with 50 fM silica spheres (310 nm diam.) and either 1, 5, or 50 mM KCl as indicated. The current dropped in a sequence of many abrupt current step features in the chronoamperograms recorded in 1 and 5 mM KCl. No step features were seen in the absence of silica spheres, and we have attributed the steps to the effect of blocking of FcMeOH diffusion by individual adsorbed silica spheres, as proposed by QHL for carboxylated latex beads.[1] They also established that the particle arrival rate and average current step height were linearly proportional to the working electrode current, and thus linearly proportional to the concentration of the redox mediator, FcMeOH. In Figure 1, the steady state current for ferrocenemethanol oxidation also varied slightly from run to

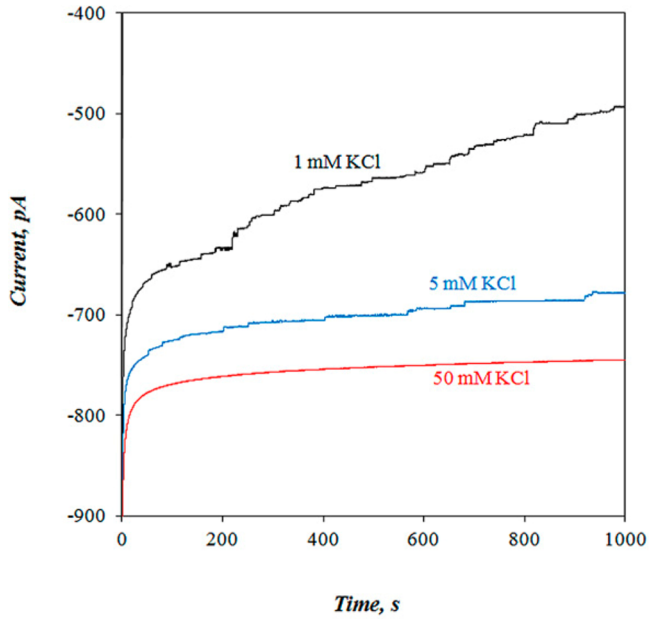

Figure 1. Chronoamperograms recorded using a 2 μm diameter Pt UME in aqueous solutions containing 2.5 mM FcMeOH, 50 fM silica spheres (310 nm diam.), and either 1 mM KCl (black), 5 mM KCl (blue), or 50 mM KCl (red) as the supporting electrolyte. The UME potential was +0.5 V vs Ag/AgCl applied at zero time.

run because of small changes in the surface area of the etched-wire UME as a result of repolishing. This produces slightly different starting currents in the three chronoamperograms before any step features appear.

The number of steps depended strongly on the concentration of supporting electrolyte. The average frequency of steps observed for the first 1000 s of data acquisition was 0.075, 0.016, and 0 Hz for 1, 5, and 50 mM KCl, respectively (while no steps were seen in the first 1000 s for 50 mM KCl, the average frequency over 5000 s was 4.0×10^{-3} Hz). Results similar to those shown in Figure 1 were also obtained for other systems containing insulating colloidal particles (unmodified polystyrene and carboxylated polystyrene spheres) in aqueous solutions with low concentration of the supporting electrolyte. A representative chronoamperogram for polystyrene sphere adsorption is shown in the Supporting Information as Figure S2.

The fact that the frequency of steps strongly depends on the supporting electrolyte concentration for all systems studied demonstrates that spheres do not move to the UME by diffusion alone. The Stokes−Einstein equation for the diffusion of spherical particles gives a diffusion coefficient of 1.4×10^{-8} cm^2/s for a 310 nm diameter sphere. Assuming irreversible adsorption of the spheres (i.e., spheres "stick" and are not expected to readily leave the surface and return to solution), the frequency of sphere arrival by diffusive flux alone is given by

$$f_{diff} = 4D_sC_sr_0 \quad (1)$$

where f_{diff} is the frequency of sphere arrivals due to diffusion, D_s is the diffusion coefficient of the spheres as calculated from the Stokes−Einstein equation in cm^2/s, C_s is the number concentration of spheres in particles/cm^3, and r_0 is the radius of the working electrode in cm.[11,12] For the 2 μm diameter UME, this would predict a sphere arrival frequency of only 1.7 $\times 10^{-4}$ Hz, nearly 3 orders of magnitude smaller than the step

frequencies observed for experiments in solutions containing 1 or 5 mM KCl. These considerations, which are also in agreement with the report by QHL, suggest that the particles arrive at the UME by migration. Moreover, we have measured the ζ-potential of the silica spheres as −58.9 mV using dynamic light scattering. The same experiment also measured the electrophoretic mobility of the spheres as -4.617×10^{-8} $m^2/(V\,s)$. This mobility value is in good agreement with the theoretical values reported in the literature.[18,19] Thus, under FcMeOH oxidation current, the spheres are able to migrate toward the working electrode due to their negative surface charge, which is imparted by surface silanol moieties for the silica spheres.[20]

The magnitudes of the current steps showed an interesting time dependence (criteria for identifying steps are discussed in the Materials and Instrumentation section). As shown in Figure 2 and Figure S3 in the Supporting Information, the height of the current steps was essentially independent of time and step frequency at short times (the first few hundred seconds of each chronoamperometric run). This is consistent with the interpretation that the spheres are adsorbing onto pristine sites on the Pt surface at submonolayer coverage. As will be developed further in the theoretical sections below, variation in the current step heights at submonolayer coverage is attributed to landing of the spheres on different regions of the electrode with different current densities, because the diffusive flux of FcMeOH (and thus, blocking by the spheres) is greater at the edge of the disk electrode than at the center.[21]

At long times (approaching 1000 s and longer), the average height of the current steps decreased, reflecting adsorption of the spheres at greater than monolayer coverage as the electrode current becomes dominated by diffusion to voids in the adsorbed sphere layer. This is shown clearly in the inset of Figure 2, where the size of the individual current steps for the 1 mM KCl case continues to decrease until the current approaches a limiting value of roughly 60% of the diffusion limited current observed in the absence of the spheres. As this step current decrease is tied to the surface coverage of adsorbed spheres, it is most readily observed at low supporting electrolyte concentration where the number of sphere arrivals is higher. For the 1 mM KCl case, the average positive step height decreased from 2.2 pA in the first 1000 s of the 5000 s chronoamperogram to 0.35 pA for the 4000−5000 s interval. For the 5 mM KCl case, the average step height decreased from 2.7 pA in the first 1000 s to 1.4 pA in the last 1000 s. No apparent decrease in step heights was observed in the 50 mM KCl case due to the much smaller number of sphere arrivals at the electrode. It should be noted that similar trends were also observed for both polystyrene particle systems. Importantly, the instrument noise level prevented steps smaller than ∼300 fA from being resolved, and there may be additional adsorption events occurring at longer times which were not recorded in the chronoamperogram due to their smaller effect on the overall current, particularly in the 1 mM KCl case. When spheres were injected to the cell at much higher concentrations (1 pM or greater), maximal blocking was reached almost immediately, and the step events disappeared completely by the end of the chronoamperogram (see the Supporting Information).

The results of the experiments presented in Figures 1 and 2 (and Figures S2 and S3 in the Supporting Information) became clearer after performing numerical simulations of the observed phenomena. In particular, we investigated the effect of blocking of the flux of FcMeOH by adsorbed insulating spheres as well as the mass transfer of spheres by migration using two theoretical models. The first simulated the magnitude of current steps, while the second simulated the flux of the particles at the electrode and thereby the frequency of their collisions with the electrode surface.

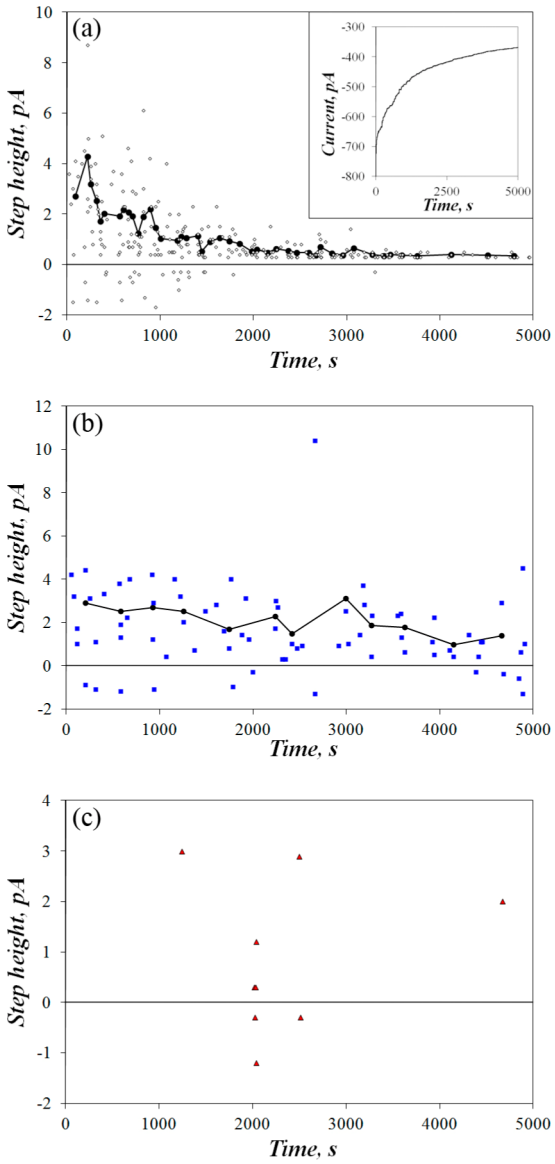

Figure 2. Plot of the magnitude of individual current step events during 5000 s chronoamperograms recorded using a 2 μm diameter Pt UME in aqueous solutions containing 2.5 mM FcMeOH, 50 fM silica spheres (310 nm diam.), and either (a) 1 mM KCl, (b) 5 mM KCl, or (c) 50 mM KCl as the supporting electrolyte. Each data point reflects the height of one current step event, and the connected black dots in parts a and b show a moving average of every five positive steps. Positively signed steps indicate a decrease in FcMeOH oxidation current (more blocking of FcMeOH diffusion), while negatively signed steps indicate an increase in FcMeOH oxidation current (less blocking of FcMeOH diffusion). Instrumental noise prevented discrimination of steps below 300 fA. Inset in part a: Raw chronoamperogram for the 1 mM KCl case, showing eventual near-maximal blocking due to the adsorbed spheres.

Numerical Simulation of Current Steps due to Blocking of Electrode by Insulating Particles. The simulation discussed here was done using the Convection and Diffusion application mode of Multiphysics v3.5a (Comsol,

Stockholm, Sweden). The procedure consisted of two parts: in the first part, the steady-state current was calculated and compared to an analytical solution for a disk electrode,[21] and in the second part, the current was calculated assuming the presence of an insulating body on the disk surface. Thereby, it was possible to calculate the change in the faradaic current due to the adsorption of a single insulating particle at the electrode surface.

The Nernst−Planck equation, which is solved numerically, can be written assuming diffusional and migrational mass transfer modes as

$$J_i(r, z) = -D_i \nabla C_i(r, z) - \frac{z_i F}{RT} D_i C_i(r, z) \nabla \varphi(r, z) \quad (2)$$

where J is the flux of the species i, D is the diffusion coefficient, C is the concentration, z is the charge on the species in signed units of electronic charge, F is the Faraday constant, φ is the electric potential responsible for the migration effect, and other symbols have their usual meaning.

Other relevant equations, including the initial and boundary conditions, are described in the Supporting Information. The geometry of the model used in the simulations is shown in Figure S7 in the Supporting Information. Note that, if the meshing of the geometry is not sufficiently fine, then the numerical solution for the limiting current through the disk differs from the analytical by more than 0.4% (ca. 8 pA for a 2.5 μm radius electrode and 2 mM concentration of the redox species). This creates a problem, since the simulated change in the faradaic current due to blocking by a single NP (the magnitude of the current step) is then comparable to the simulation error. Therefore, to improve the accuracy of the calculations within the multiphysics environment, we have simulated the change in the current due to the presence of an insulating ring rather than a particle. The number of spherical particles (N) that "fit" into the ring is given by the following equation:

$$N = \frac{3\pi}{2}\left(\frac{r}{a}\right) \quad (3)$$

where a is the particle radius and r is the distance from the disk center to the particle position on the electrode surface.

Consequently, the magnitude of a step due to a single NP (I_s) is equal to the value for the ring (I_r) divided by the number of particles in the ring:

$$I_s = \frac{I_r}{N} \quad (4)$$

The results of the simulations indicate that the magnitude of the observed current steps depends on a number of factors, such as the concentration of the redox species, i.e., FcMeOH, the size of both the particle and the electrode, and the particle landing position on the electrode surface. The flux of FcMeOH toward the electrode is directly proportional to the FcMeOH concentration. Therefore, the magnitude of a current step due to the flux blockage by a particle will also be directly proportional to the concentration of FcMeOH; this is supported by the results of the simulations shown in Figure 3 and the experimental data in Figure S4 in the Supporting Information. According to the histograms in Figure S4 in the Supporting Information, the magnitude of the largest current steps decreased from about 5.5−6 to 2.5−3 pA when the concentration of the redox species dropped from 2 to 1 mM; the number of smallest current steps (0.5 pA), however, increased.

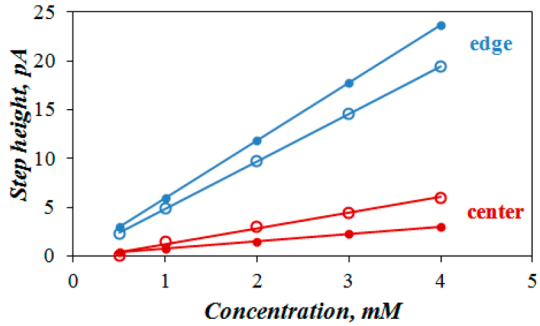

Figure 3. Effect of the redox species concentration (FcMeOH) and particle location (edge vs center) on the magnitude of current steps due to adsorption of one insulating particle. Blue data points represent simulation results for a particle adsorbed at the edge of the electrode, while red shows that for a particle located close to the electrode center. Electrode radius: 1 μm (open circles) and 2.5 μm (full circles). Particle radius: 155 nm (open circles) and 260 nm (full circles).

To a first approximation, the relative size of the particle with respect to the electrode determines how much the flux of FcMeOH to the electrode will decrease. This agrees well with the simulated data in Figure 4; i.e., the bigger the particle, the larger the current step due to the flux blockage, all other conditions remaining the same. However, a complication arises here from the fact that the particle landing position also affects the magnitude of the current step. In Figure 5, the relative change in the faradaic current due to the adsorption of an insulating particle is plotted as a function of the distance from the disk center; the magnitude of the current step increases when the particle lands closer to the electrode edge. This is because the flux of the redox species (FcMeOH) is much higher at the edge of the electrode than at its center, and therefore, the particle blocks the flux of FcMeOH to a larger extent when it adsorbs closer to the edge.

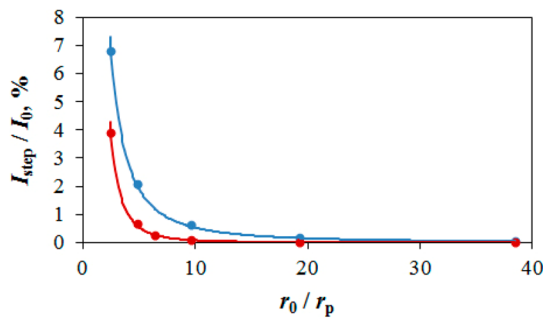

Figure 4. Effect of normalized particle size (r_p = particle radius, r_0 = disk electrode radius) on the magnitude of current steps (presented as the percent of the current through the disk). Simulations were done assuming particle adsorption either at the electrode edge (blue data points) or at the center of the electrode (red data points).

The solid curve in Figure 5 corresponds to the normalized flux of FcMeOH at the electrode disk, and the data points correspond to the magnitude of current steps. Thus, the change in the current step magnitude follows the change in the flux of the redox species. In addition, for the same ratio r_0/r_p, it is possible to correlate the position where a particle lands on the electrode surface to the magnitude of the current step observed

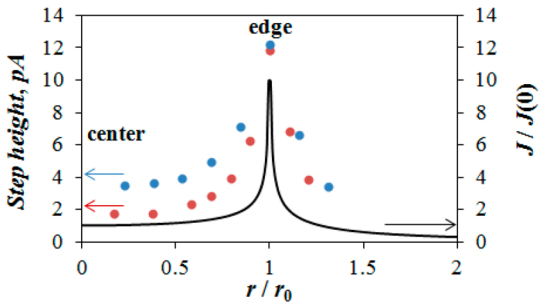

Figure 5. Magnitude of current steps (data points) as a function of the normalized distance from the electrode disk center (particle landing position). The black curve represents the normalized flux of the redox species through the disk. Simulations were done for (red points) an electrode disk radius r_0 of 2.5 μm, a particle radius of 260 nm, and a FcMeOH concentration of 2 mM and (blue points) an electrode disk radius r_0 of 1 μm, a particle radius of 155 nm, and a FcMeOH concentration of 2.5 mM.

in the collision experiment. Note that $r/r_0 > 1$ represents particles landing on the insulator sheath surrounding the electrode and that even particles landing in this region cause a perturbation of the current (because mass transfer involves spherical coordinates).

The wide variation in the current step magnitudes observed in collision experiments may be understood as a combined effect of the relative particle/electrode diameters and the edge contribution to the flux of the redox species. Histograms of recorded step heights for both silica and polystyrene sphere adsorption experiments (see Figures S4 and S5 in the Supporting Information) show a distribution agreeing well with the behavior predicted in Figure 5. However, one can notice that a substantial number of collisions have magnitudes less than 1 pA. These current steps are believed to be due to collisions of particles at greater than monolayer coverage (i.e., multilayer formation) or due to adsorption of the particles to the glass sheath in the immediate vicinity to the electrode edge (as shown in Figure 5, where such collisions still lead to flux blockage). Such small steps may also be due to rearrangement of the spheres on the surface, as described below.

Numerical Simulation of Mass Transport of Insulating Particles to the Working Electrode. The simulations of the flux of the insulating particles were carried out using the Nernst−Planck with electroneutrality (NPE) application mode of the Chemical Engineering Module in Multiphysics v3.5a. The two general equations solved were the Nernst−Planck equation (eq 2) and the electroneutrality condition (eq 5):

$$\sum_i z_i C_i = 0 \tag{5}$$

where z is the charge and C is the concentration of all species in the system.

These two equations apply to the redox species (A and A^+), the supporting electrolyte ions (K^+, Cl^-), as well as the negatively charged NPs. Oxidation of FcMeOH (A), which occurs on the working electrode, leads to the formation of a charged species (hydroxymethylferrocenium ion, A^+). Uncharged FcMeOH only arrives at the electrode by diffusion; however, the electric field is responsible for the migration of the charged NPs. If the concentration of supporting electrolyte is low, then this field will substantially affect the concentration of all charged species in the system, particularly near the working electrode. Therefore, in addition to the diffusive mode of mass transport (first term in eq 2), we need to consider the migration of ions and particles (second term in the equation). The electroneutrality condition (eq 5) requires that in any volume element of solution the number of positive and negative species are equal. Indeed, this is the case in our model, since we do not consider the presence of the double layer (or space charge region) near the electrode. The use of the electroneutrality condition is required so that the number of unknowns and solved equations are equal. A discussion of the initial and boundary conditions used in the NPE model, as well as all other relevant equations is given in the Supporting Information. For further details regarding the NPE approach in simulations of the migration effect, the interested reader is referred to the works by Oldham and Feldberg.[22,23]

In Figure 6a, one can see the simulated distribution of the electric field near a disk UME in a solution with a low concentration of the supporting electrolyte. As expected, the strength of the field is much higher at the edge of the electrode.[24] We believe this is also the reason why studied insulating particles adsorb preferentially to the electrode surface closer to the edge of the disk rather than to its center. Note

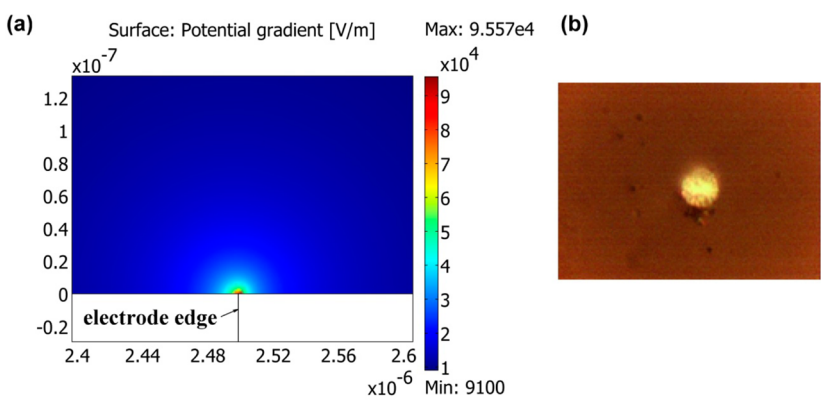

Figure 6. (a) Simulated distribution of the electric potential gradient near the electrode showing the presence of the edge effect. Simulations were done for the 2.5 μm radius disk electrode in 2 mM FcMeOH and 1 mM KCl. The potential applied to the electrode was +0.45 V, which corresponded to diffusion limited steady-state oxidation of FcMeOH. (b) The photograph of a 2.5 μm radius disk electrode taken after a polystyrene particle adsorption chronoamperogram was recorded (t < 1000 s). The size of the particles was 520 nm and the concentration 50 fM. Other conditions of the experiment were the same as described in part a.

there are two effects of the field, one contributing to migration (mass transfer) of the particle and another contributing to the sticking of the particle to the electrode on arrival. Figures 6b and S8 (Supporting Information) show the results of visual observations (in situ and ex situ photographs) of an experiment involving the adsorption of negatively charged polystyrene particles on a 2.5 μm radius disk Pt UME. In the beginning of the experiment (Figure S8, Supporting Information, t = 4 min), one can definitely see a number of particles that adsorbed close to the edge of the electrode. With time, the number of adsorbed particles increased (Figure S8, Supporting Information, t = 15 min). Once the experiment was stopped and the electrode was examined ex situ under an optical microscope, a clear distribution of the particles around the edge of the electrode was noticed (Figure 6b). Although one cannot completely neglect the possibility that some of the particles may have been dislodged during the removal of the solution, the results in Figure 6b and Figure S8 in the Supporting Information quite convincingly suggest that the particles adsorb closer to the edge of the electrode disk due to the edge effect.

To further support the assertion that migration is the dominant mode of transport of particles, we investigated the effects of the supporting electrolyte concentration and the FcMeOH oxidation current (as set by the working electrode potential) on the magnitude of the electric field and, subsequently, the frequency of particle collisions. The results of these investigations are shown in Table 1. In these data, the uncertainty in the simulated collision frequency value accounts for the uncertainty in the experimentally measured zeta potential, while the uncertainty in the experimental value of the collision frequency is the standard deviation obtained from three measurements. The data in Table 1 show that, as the concentration of KCl in the cell is increased, the frequency of collisions decreases for all other parameters being equal. These results can be understood in that an increase in the supporting electrolyte concentration decreases the strength of the electric field responsible for migration. Therefore, the frequency of sphere arrivals drops with increasing supporting electrolyte concentration.

The data presented in Table 1 also indicates that the FcMeOH oxidation current, as set by the working electrode potential, also determined the rate of transfer of the particles to the electrode. This effect can be explained by the change in the strength of the electric field causing the migration of ions and particles: the field becomes weaker once the working electrode potential was stepped to less positive values than the potential for the diffusion limited steady-state oxidation of FcMeOH. As a result, at the half-wave potential of FcMeOH oxidation (+0.28 V), the frequency of particle collisions was also approximately one-half of that observed at +0.45 V (potential of the diffusion limited steady-state oxidation of FcMeOH).

Simulations of the frequency of insulating particle collisions indicated that the developed model is sufficiently accurate and robust, and does not contain any adjustable parameters. Some discrepancy between the theoretical and experimental values of the collision frequency can be attributed to the inevitable errors in the experimental measurements of the zeta potential of particles and the collision frequency (especially toward the end of experiments when the particle multilayer formation occurs and the magnitude of current steps decreases significantly). The model currently assumes that the arrival of all insulating particles by migration results in their irreversible adsorption to the electrode surface ("sticking"). This may not be the case for all studied systems, since the exact nature of the interaction between a particle and the electrode surface is not yet well understood.

Dynamics of Particle Adsorption. Analysis of individual current steps on collision curves suggests that the adsorption of particles happens rather quickly. In most cases, current step features occurred over time scales shorter than the experimental sample rate (33 and 100 ms for silica and polystyrene adsorption experiments, respectively). We estimated the distance the particle traveled during this time and the extent of blocking before the particle contacted the electrode by simulating the change in faradaic current for a number of geometries, in which the distance between the particle and the disk electrode varied between 0 and 3.9 μm. The results of these simulations are presented in Figure 7. The results show little blocking effect for $z/r_0 > 10$.

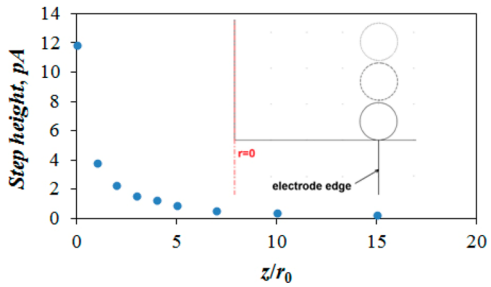

Figure 7. Current step magnitude as a function of the distance of a particle from the electrode surface, z. Simulations were performed assuming a geometry with a particle center located on the plane going through the edge of the electrode perpendicular to its surface (similar to the one shown in the inset and in Figure S7, Supporting Information), while the distance between the particle and the edge varied between 0 and 3.9 μm (r_0 = 260 nm is the particle radius). The concentration of the redox species was 2 mM.

A simple estimate based on an equation for the root-mean-square displacement (eq 6) suggests that, for a 520 nm particle, it would take about 10 s to travel the same distance (3.9 μm) by diffusion only:

$$t = \frac{(\bar{\Delta})^2}{2D_p} \tag{6}$$

where $\bar{\Delta}$ is the rms displacement of the particle due to its diffusion. This value is over 2 orders of magnitude larger than what was observed in the experiments and, in line with the frequency simulation results, is a confirmation that migration is the dominant mode of particle transport under the experimental conditions. One could further use particle mobility (about 5×10^{-8} m^2 V^{-1} s^{-1}) and the electric field strength values (on the order 10^4–10^5 V/m, Table 1) to approximate the travel time for the discussed distance 3.9 μm to be on the order of 1–10 ms.

Other Features of Sphere Adsorption Chronoamperograms. In addition to the features considered above in the chronoamperograms, which were interpreted as the arrival of single spheres at the UME by electrophoretic migration, with irreversible adsorption ("sticking") to the surface at a given location and blocking diffusion of FcMeOH to the electrode, other features were occasionally seen that might provide insight into details of possible single particle events. While the "descending staircase" of irreversible step features dominated

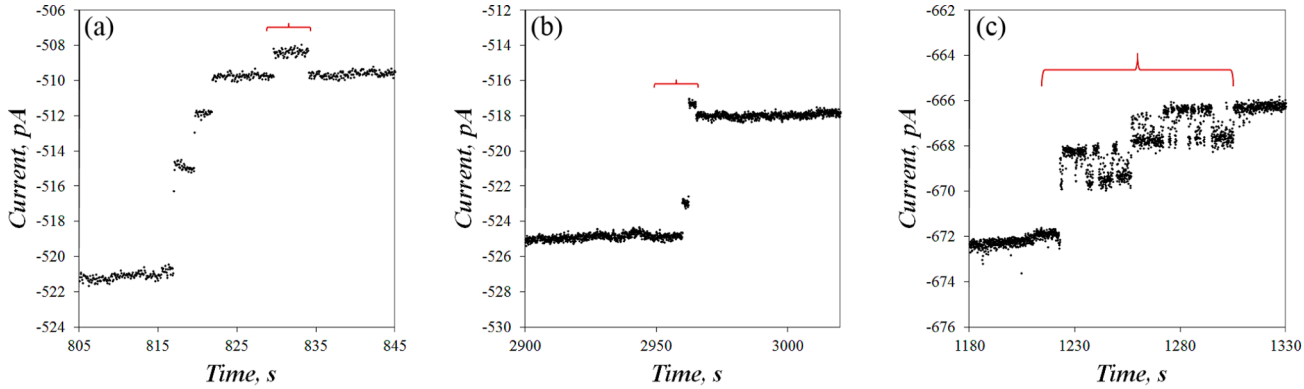

Figure 8. Highlighted features found in chronoamperograms for adsorption of 310 nm diameter silica spheres at a 2 μm Pt UME in 2.5 mM FcMeOH: (a) spontaneous desorption of a particle, with 50 fM silica spheres and 1 mM KCl; (b) coupled blocking events, with 5 fM silica spheres and 1 mM KCl; (c) apparent instability of one or more adsorbed spheres on the electrode, with 50 fM silica spheres and 5 mM KCl.

the observed changes to the mass transfer limited current (>90% of steps), additional different looking features were also observed. These might signal such events as particle desorption, interactions of pairs of particles, or motion of an adsorbed particle on the surface. Three such features are shown in Figure 8. Figure 8a is an example of a current step (1.3 pA) that is followed in less than 5 s by a step of opposite sign and equal magnitude, returning the electrode current to its previous value. This event might show an adsorption event followed by spontaneous desorption of a single particle from the electrode.

For all experiments in solutions containing 50 fM spheres, we often observed a series of several (two to four) steps bunched together over a small time interval (<2 s between steps). We also commonly observed small (<1 pA), negatively signed current steps that closely followed (<5 s) larger (2−3 pA), positively signed steps, with no oppositely signed counterpart apparent, as was in Figure 8a. To explore the possibility that these close steps may in fact be coupled events, rather than simply the effects of two independent particles on the electrode surface, we carried out chronoamperometry in solutions containing 2.5 mM FcMeOH, 1 mM KCl, and 5 fM spheres (chronoamperograms shown in the Supporting Information). At this lower concentration of spheres, roughly 14% as many step events were seen vs an experiment with 50 fM spheres. Groups of "coupled" steps were still observed in this case, and one representative example is shown in Figure 8b. The group of steps highlighted by brackets in the figure consists of three step features with heights of 1.9, 5.6, and −0.6 pA, occurring over less than 6 s.

A simple statistical test of the probability of simultaneous collisions of independent particles can help establish whether such "step-bunches" are in fact coupled events, e.g., involving one sphere moving to different locations on the electrode surface or by two or more physically coupled spheres in solution. If we first remove from consideration all clear "adsorption/desorption pairs" of steps (as in Figure 8a), the total remaining step events (positive or negative) divided by the experiment time yielded an overall frequency of possibly related electrode events in the experiment. During two identical 5000 s adsorption experiments with a 5 fM sphere concentration, the average overall frequency of nonpaired steps was 0.013 Hz. Importantly, with 5 fM spheres, almost no decrease of the step height was observed over 5000 s, and the recorded step frequency remained reasonably constant over the entire experiment. For these two experiments, we observed five instances of groups of three steps spaced less than 6 s apart.

The probability of the chance near simultaneous collision of two independent particles may be treated using a Poisson distribution by

$$P(x{=}k) = \frac{\lambda^k e^{-\lambda}}{k!} \tag{7}$$

where $P(x{=}k)$ is the Poisson probability that exactly k stochastic events will occur during a specified time interval, given an average rate of events occurring, λ.[25] If the overall step event frequency in Hz is taken as the probability that a given 1 s interval will contain one event, then it follows that, for λ = 0.076 (0.013 Hz × 6 s), one calculates a probability of 7.3×10^{-5} that a given 6 s interval will contain exactly three steps ($P(x{=}3)$). Summing this with terms for $P(x{>}3)$, one calculates an approximate cumulative probability, $P(x{\geq}3)$, of 7.6×10^{-5} that a given 6 s interval in the experiment will contain three or more steps. Thus, the average rate of occurrence for these "bunches" of three or more steps should be 0.13 per 10 000 s (or two 5000 s experiments). Performing an additional calculation now with λ = 0.13, one calculates a probability of 2.7×10^{-7} (0.000 027%) that over 10 000 s of chronoamperometric data we would record five or more such "bunches" from independent particles. While this test does not explain the physical meaning of these step-bunches, it does strongly suggest a nonstochastic character in the data, i.e., at least some of the step events recorded are not independent of one another. Therefore, to explain the repeated observation of these unlikely step spacings, we suggest that many of the closely spaced steps reflect not adsorption/desorption events of independent spheres but rather reorganization/settling of single spheres or groups of physically coupled spheres. Considering the large difference in blocking of diffusive flux of redox species by spheres adsorbed at the electrode center versus those adsorbed at the edge, it is possible that a particle impacting at one site on the electrode moves to another site by thermal motion or other disturbance before stopping at a more stable site.

Finally, we have also occasionally observed instances where the diffusion limited current during sphere adsorption showed many densely spaced transients or oscillated between two values repeatedly, as shown in Figure 8c. We suggest that these events may reflect instability or dynamic rearrangement of one sphere or groups of spheres on the electrode surface, and we chose not to count these rapidly oscillating features in the

determination of step frequency to avoid "recounting" single spheres in our arrival rates. Figure 8c shows an example of oscillation between two current levels. Such spiking/oscillating behavior was also noted by QHL for the adsorption of 300 nm diameter carboxylated latex beads and 50 nm diameter CdSe spheres but not 1 μm diameter carboxylated latex beads. This difference in behavior between the two particle sizes was attributed to the increasing effect of Brownian motion on the spheres as their size decreased.

CONCLUSIONS

The adsorption events of individual sub-μm silica and polystyrene NPs at UMEs were monitored by their blocking of FcMeOH diffusion to the electrode surface. The current-blocking corresponding to each particle adsorption event as well the frequency of particle arrivals at the electrode were recorded using chronoamperometry in dilute aqueous suspensions of the spheres (fM concentrations). Numerical simulations of both blocking and arrival frequency by diffusion and migration were in good agreement with the experimental data. These findings firmly establish this diffusion-blocking approach, pioneered by QHL,[1] as a promising experimental tool within nanoscale electrochemistry for both the study of single particle/electrode collision events and also for directing the assembly of insulating particles at the electrode/electrolyte interface.

Numerical simulations of blocking events suggest that it becomes progressively harder to detect insulating particles less than 100 nm in diameter by their adsorption unless an electrode of a smaller size is used. One way of overcoming this limitation is by using a high concentration of the redox species. However, in the particular case of FcMeOH, one cannot attain concentrations above 4 mM in an aqueous solution. One could however use a more soluble redox couple to improve the sensitivity of the collision detection. As a rule of thumb, larger electrodes (10−25 μm diam.) are sufficient for experiments with larger particles (>1 μm), while smaller electrodes (<2 μm diam.) should be employed in experiments with particles less than 500 nm in size.

The use of migration for particle preconcentration can be important for the application of particle collision methods in electroanalysis. We show that the electric field established with low-electrolyte concentrations gives rise to over 3 orders of magnitude increase in the flux of charged NPs. Thus, we believe this rather simple method can be used for manipulation of important biological materials (proteins, DNA) similarly to electrophoresis, dielectrophoresis (DEP), and other electrokinetic techniques.

ASSOCIATED CONTENT

Supporting Information

Representative experimental data for polystyrene sphere adsorption experiments, histograms showing the distribution of current steps for both polystyrene and silica sphere adsorption experiments, a chronoamperogram showing injection of spheres at increased (1 pM) concentration, and detailed descriptions of the numerical simulations used to describe diffusion blocking and sphere arrival frequency. This material is available free of charge via the Internet at http://pubs.acs.org.

AUTHOR INFORMATION

Corresponding Author

*E-mail: ajbard@mail.utexas.edu.

Author Contributions

†Both authors contributed equally to this work.

Notes

The authors declare no competing financial interest.

ACKNOWLEDGMENTS

The authors thank Karole Blythe and Katherine Willets for their donation of carboxylated polystyrene and silica sphere samples used in our first experiments. The authors thank Kevin C. Leonard for his help with data analysis and potentiostat assembly. This work was supported by the Department of Defense, Defense Threat Reduction Agency (Contract No. HDTRA1-11-1-0005). The content of the information does not necessarily reflect the position or the policy of the federal government, and no official endorsement should be inferred. Additional support was provided by the Robert A. Welch Foundation (F-0021 and H-F-0037).

REFERENCES

(1) Quinn, B. M.; van't Hof, P. G.; Lemay, S. G. *J. Am. Chem. Soc.* **2004**, *126*, 8360−8361.
(2) Heyrovskỳ, M.; Jirkovskỳ, J. *Langmuir* **1994**, *11*, 4288−4292.
(3) Heyrovskỳ, M.; Jirkovskỳ, J.; Müller, B. R. *Langmuir* **1994**, *11*, 4293−4299.
(4) Heyrovskỳ, M.; Jirkovskỳ, J.; Štruplová-Bartáčková, M. *Langmuir* **1994**, *11*, 4300−4308.
(5) Heyrovskỳ, M.; Jirkovskỳ, J.; Štruplová-Bartáčková, M. *Langmuir* **1994**, *11*, 4309−4312.
(6) Hellberg, D.; Scholz, F.; Schauer, F.; Weitschies, W. *Electrochem. Commun.* **2002**, *4*, 305−309.
(7) Hellberg, D.; Scholz, F.; Schubert, F.; Lovrić, M.; Omanović, D.; Hernández, V. A.; Thede, R. *J. Phys. Chem. B* **2005**, *109*, 14715−14726.
(8) Scholz, F.; Hellberg, D.; Harnisch, F.; Hummel, A.; Hasse, U. *Electrochem. Commun.* **2004**, *6*, 929−933.
(9) Rees, N. V.; Banks, C. E.; Compton, R. G. *J. Phys. Chem. B* **2004**, *108*, 18391−18394.
(10) Clegg, A. D.; Rees, N. V.; Banks, C. E.; Compton, R. G. *ChemPhysChem* **2006**, *7*, 807−811.
(11) Xiao, X. Y.; Bard, A. J. *J. Am. Chem. Soc.* **2007**, *129*, 9610−9612.
(12) Xiao, X. Y.; Fan, F.-R. F.; Bard, A. J. *J. Am. Chem. Soc.* **2008**, *130*, 16669−16677.
(13) Kwon, S. J.; Fan, F.-R. F.; Bard, A. J. *J. Am. Chem. Soc.* **2010**, *132*, 13165−13167.
(14) Bard, A. J.; Zhou, H.; Kwon, S. J. *Isr. J. Chem.* **2010**, *50*, 267−276.
(15) Kwon, S. J.; Zhou, H.; Fan, F.-R. F.; Vorobyev, V.; Zhang, B.; Bard, A. J. *Phys. Chem. Chem. Phys.* **2011**, *13*, 5394−5402.
(16) Zhou, Y.-G.; Rees, N. V.; Compton, R. G. *Angew. Chem., Int. Ed.* **2011**, *50*, 4219−4221.
(17) Fan, F.-R. F.; Demaille, C. In *Scanning Electrochemical Microscopy*; Bard, A. J., Mirkin, M., Eds.; Marcel Dekker: New York, 2001; p 75.
(18) O'Brien, R. W.; White, L. R. *J. Chem. Soc., Faraday Trans. 2* **1978**, *74*, 1607−1626.
(19) Ohshima, H.; Healy, T. W.; White, L. R. *J. Chem. Soc., Faraday Trans. 2* **1983**, *79*, 1613−1628.
(20) Heston, W. M., Jr.; Iler, R. K.; Sears, G. W., Jr. *J. Phys. Chem.* **1960**, *64*, 147−150.
(21) Bard, A. J.; Faulkner, L. R. *Electrochemical Methods: Fundamentals and Applications*, 2nd ed.; John Wiley: New York, 2001; p 174.
(22) Oldham, K. B. *J. Electroanal. Chem.* **1988**, *250*, 1−21.

(23) Oldham, K. B.; Feldberg, S. W. *J. Phys. Chem. B* **1999**, *103*, 1699−1704.
(24) Newman, J. *J. Electrochem. Soc.* **1966**, *113*, 501−502.
(25) Bertsekas, D. P.; Tsitsikils, J. N. *Introduction to Probability*; Athena Scientific: Belmont, MA, 2002; p 78.